# DIGITALES ARCHIV

Ospino-Castro, Adalberto; Navas, Sharys Romero; Robles-Algarín, Carlos

**Article**

# Methodology for generating a reference wind year for offshore wind energy : a case study in La Guajira, Colombia

**Provided in Cooperation with:**
International Journal of Energy Economics and Policy (IJEEP)

This Version is available at:
http://hdl.handle.net/11159/701607

# Methodology for Generating a Reference Wind Year for Offshore Wind Energy: A Case Study in La Guajira, Colombia

Adalberto Ospino-Castro[1]*, Sharys Romero Navas[1], Carlos Robles-Algarín[2]*

[1]Universidad de la Costa, Barranquilla, Colombia, [2]Universidad del Magdalena, Santa Marta, Colombia.
*Email: aospino8@cuc.edu.co, croblesa@unimagdalena.edu.co

**ABSTRACT**

Due to its excellent potential, wind power has gained importance as a renewable energy source in Colombia, especially in the offshore Caribbean region. However, one of the main challenges in the development of offshore wind projects is the analysis of the wind resource. This study presents the generation of a specific typical meteorological year (TMY) for wind energy in the Colombian Caribbean region, known in the literature as Reference Wind Year (RWY). The methodology used was based on the Sandia method, widely accepted in the analysis of wind resources. A comparison between the cumulative distribution function (CDF) and the statistic approach Finkelstein-Schafer (FS) was applied to evaluate multiple meteorological parameters in the study area associated with wind resource potential assessment, such as wind speed and direction, temperature and atmospheric pressure, compiled for 10 years (2012-2021). The representative years were weighted according to their importance and combined into a dataset. The results indicated that the proposed method was able to generate highly representative and accurate data for the case study in La Guajira, Colombia, guaranteeing its suitability for implementation in other locations with different climatic conditions.

**Keywords:** Offshore Wind, Typical Meteorological Year, Reference Wind Year, Finkelstein-Schafer Statistics, Sandia Method
**JEL Classifications:** Q20, Q42, P18, O21

## 1. INTRODUCTION

Wind energy has emerged as a promising renewable energy source worldwide in the past few decades, and this trend is expected to continue in the coming years (Xiang et al., 2024). Colombia, a country characterized by its geographical and climatic diversity, has awakened a growing interest in the use of wind as an energy resource due to its economic, environmental and social potential (Soto Gutiérrez, 2016), thus contributing to the diversification of the energy matrix (Arce and Bayne, 2020). The country has winds cataloged as the best in South America, especially in the offshore Caribbean region, due to an advantageous geographic location with the presence of northeast trade winds (Costoya et al., 2019), which are categorized as class 7, with wind speeds above 9 m/s (Vergara et al., 2010). These wind characteristics create favorable conditions for the

development of the offshore wind energy, as reported by (Rueda-Bayona et al., 2019).

As the world moves towards a more sustainable future, wind energy has become a fundamental component of the energy landscape, particularly leveraging the offshore wind resources of the Colombian Caribbean (Arce and Bayne, 2020). Consequently, the potential of offshore wind energy has been subject to analysis on multiple occasions (Bautista Sánchez and Rojas Castellanos, 2019; Bethel, 2021; Carvajal-Romo et al., 2019), underscoring the necessity for further comprehensive analysis to advance wind energy development in the country (Soto Gutiérrez, 2016). Specifically, the northern offshore region of the country has emerged as the focal point of the energy transition, with an offshore wind potential estimated at 50GW (The Renewables Consulting Group and ERM, 2022), and projected installed capacities of

1GW by 2030, 3 GW by 2040 and 9 GW by 2050, as outlined in (Minenergia, 2022).

One of the biggest challenges when developing an offshore wind energy project is the analysis of the wind resource, which is essential due to its direct impact on the efficiency and profitability of the project (Bethel, 2021). This analysis can be conducted in a variety of ways but requires a dataset that reflects the behavior of meteorological variables to assess and project wind behavior at specific locations. This dataset is known as a Typical Meteorological Year (TMY) and has sometimes been applied to the study of wind resources, as proposed by Eikrem et al. (2023). In this study, the minimization of energy costs and the increase of annual energy production in the planning of an offshore wind farm in Portugal were predicted by constructing a TMY based on data from 10 years.

The generation of a Typical Meteorological Year (TMY) is a tool widely used in studies related to solar energy and building energy analysis. It consists of a set of hourly values of meteorological parameters specific to a given geographical location, derived from a long-term observational database and synthesized into a representative meteorological sequence for a significant year. This technique has been extensively documented in the scientific literature across various locations, including Tripoli (Alargt et al., 2021), Hong Kong (Chan et al., 2006), Togo (Patchali et al., 2022) (Amega et al., 2022), Argentina (Bre and Fachinotti, 2016), Cyprus (Kalogirou, 2003), Greece (Kambezidis et al., 2020), Turkey (Pusat et al., 2015), China (Li et al., 2020), Syria (Skeiker, 2004), Iran (Ebrahimpour and Maerefat, 2010), Ecuador (Rodríguez et al., 2019), Australia (Maklad, 2014), Portugal (Abreu et al., 2018) and Nigeria (Ohunakin et al., 2013).

The most widely accepted method in this area is the Sandia method, which was conceived for the National Renewable Energy Laboratory (NREL) (Gai et al., 2024). This method is based on the Finkelstein-Schafer (FS) statistical approach. Different authors have highlighted its relevance while comparing the generation of TMY with different methods, concluding that it is the most accurate in terms of meteorological representation (Amega et al., 2022; Kambezidis et al., 2020).

In the context of wind energy, TMYs serve as a reference for generating wind rose diagrams and conducting wind profile analysis, as demonstrated in case studies conducted in Ethiopia (Mansani et al., 2021), India (Hampannavar et al., 2021; Himabindu et al., 2021), Palestine (De Meij et al., 2016) and Tunisia (Attig-Bahar et al., 2021). However, literature suggests that TMYs used in wind energy applications should be specifically generated for this purpose (Alonso-Suárez et al., 2019). This is because many TMYs developed in specialized secondary databases tend to prioritize solar-related parameters, neglecting variables crucial for wind energy analysis such as wind speed (WS), wind direction (WD), temperature (T), atmospheric pressure (AP) and relative humidity (RH). As a consequence, these TMYs may not accurately reflect wind behavior, making it challenging to perform precise wind potential projections.

In this regard, the generation of specific TMYs, focusing exclusively on wind power analysis, has been studied on a limited scale. Initially, in the context of onshore wind power, Kotroni et al. (2014) assessed the most representative years in terms of wind to establish a typical year in Greece. Furthermore, Pusat and Karagöz (2021) proposed a novel model based on TMYs for long-term wind resource prediction at a particular location, incorporating key criteria such as wind speed, wind direction, temperature and atmospheric pressure, termed as Reference Wind Year (RWY). They employed the FS method and presented a case study in Turkey to validate their model, which forms part of the methodology referenced in this research. This approach was further supported by the investigation conducted by Karamanski and Erfort (2023), who utilized the RWY to examine both onshore and offshore wind potential along the coast of South Africa. Additionally, they calculated capacity factors and identified areas with the greatest potential for wind power generation projects.

In this scenario, the generation of datasets like the RWY becomes crucial for conducting a thorough evaluation and forecasting of wind resources in designated areas earmarked for these projects. In the Colombian context, a single application of TMY has been documented for the analysis of a photovoltaic plant in La Guajira, Colombia (Gemignani et al., 2017). Nevertheless, it is important to highlight that Colombia currently lacks an RWY specifically tailored for assessing offshore wind potential, which stands as one of the fundamental aims of this ongoing research. The step-by-step process of the selected methodology for implementing RWY is shown in Figure 1.

## 2. MATERIALS AND METHODS

For this study, 5 zones with offshore wind potential in the Colombian Caribbean region were chosen based on a prioritization of economic, environmental, technical and socio-political criteria. The results of this prioritization phase were published by the authors in Ospino-Castro et al. (2023). These zones have been identified as having significant wind resource potential, as confirmed by Rueda-Bayona et al. (2019). Figure 2 and Table 1 provide the coordinates and locations of these selected zones. This paper focuses on presenting the case study of Zone 1, situated in the municipality of Uribia, in the department of La Guajira.

The NASA ERA-5 database was utilized to analyze the meteorological variables WS, WD, T and AP at a height of 10 meters over a period of 10 years, spanning from 2012 to 2021. This period includes 3 leap years (2012, 2016, 2020). The methodology employed for generating the RWY, based on the study proposed by Pusat and Karagöz (2021), draws upon the traditional TMY generation method developed by Hall et al. (1978). This method involves selecting representative meteorological data from various years within the evaluated timeframe, resulting in 12 typical meteorological months (TMM).

This selection process involves comparing the cumulative distribution function (CDF) of each month for each year to determine their absolute closeness to the long-term behavior

**Figure 1:** Graphical methodology for the application of RWY
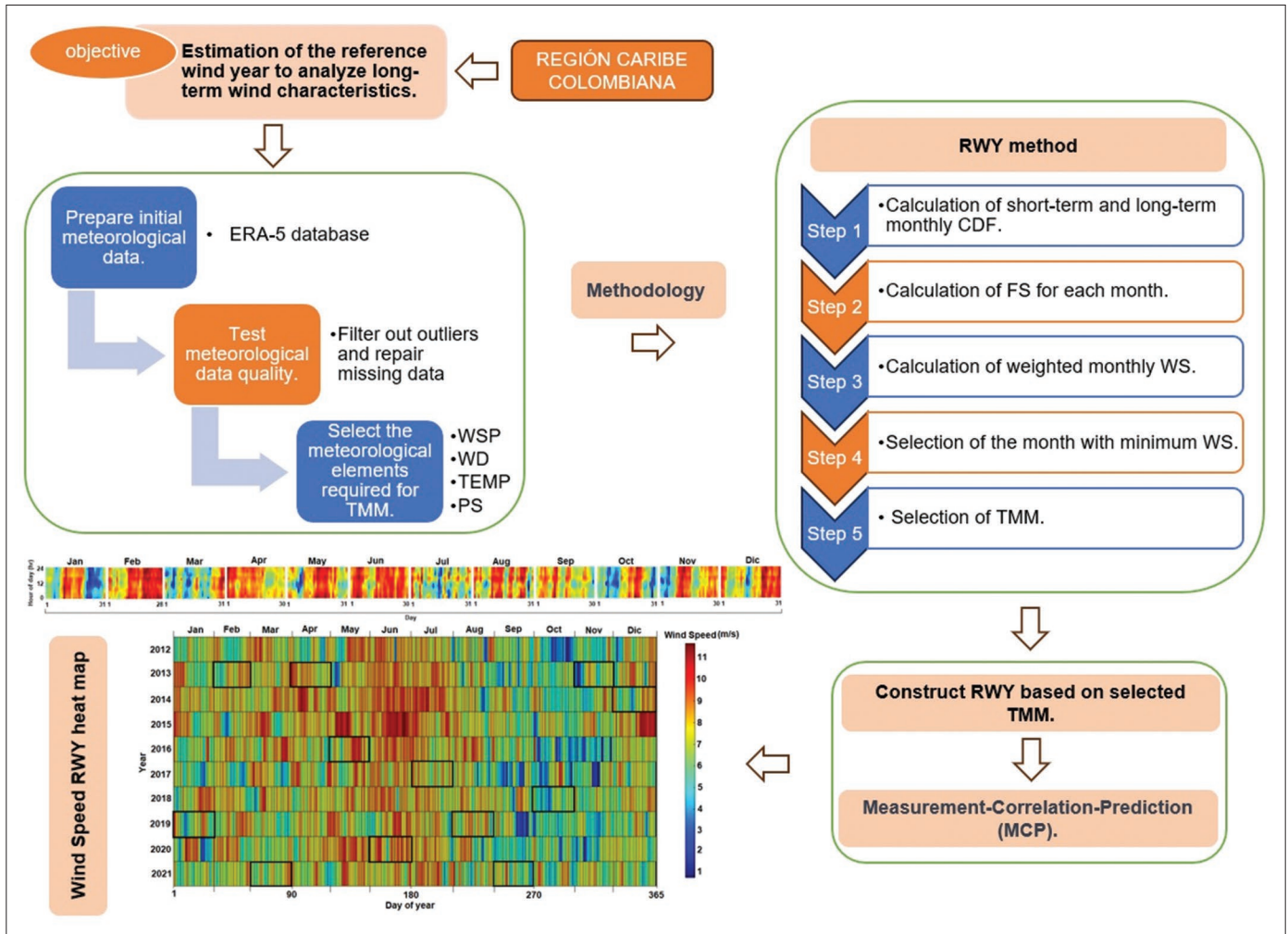


**Figure 2:** Location of selected offshore zones in the Colombian Caribbean region
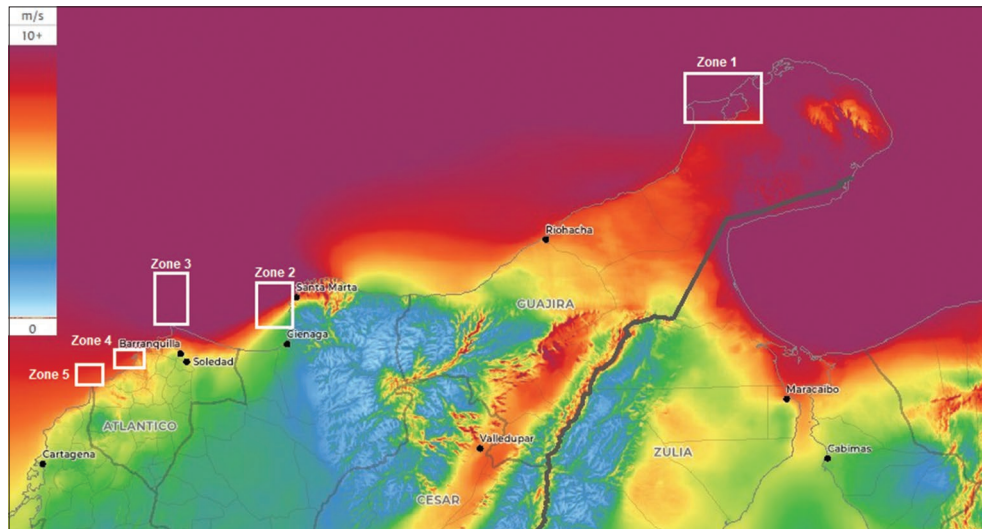


observed over the 10-year study period. Through this analysis, 5 candidate years are selected by evaluating the relative function of the intervals determined for each meteorological parameter. The CDF in this context corresponds to the relative frequency, as defined by Eq. (1).

$$f_i = \left( \frac{N_{(a,b)}}{n} \right) \tag{1}$$

Where $N_{(a,b)}$ is the function that counts the intervals, $n$ represents the amount of data in the set, $x_i$ is the value of the wind speed at the

evaluated instant, and $I(x_i \in [a,b])$ corresponds to the mathematical function given in Eq. (2).

$$N_{(a,b)} = \sum_{i=1}^{n} I(x_i \in [a,b]) \tag{2}$$

$$\begin{cases} 1 \, si \, x_i \in [a,b] \\ 0 \, si \, x_i \notin [a,b] \end{cases}$$

In this manner, the function increments by 1 for each data point falling within the interval of the evaluated meteorological parameter. Consequently, it indicates the number of intervals that satisfy the condition stipulated in Eq. (3).

$$F_i = \frac{N_i}{n} = f_1 + f_2 + \ldots + f_i = \sum_{j=1}^{i} f_j \tag{3}$$

The Finkelstein-Schafer (FS) statistical method serves as the tool for analyzing absolute closeness, and it is computed using Eq. (4).

$$FS = \left(\frac{1}{n}\right) \sum_{i=1}^{n} \delta_i \tag{4}$$

Where $\delta_i$ corresponds to the absolute difference between the cumulative distribution function (CDF) of the 10 years evaluated and the CDF for each year, in the month evaluated, for each day represented by $i$, and $n$ corresponds to the number of daily records for the month evaluated. For the appropriate selection of each typical month concerning the calculated FS, weighting factors (WF) are determined. Each index is assigned a statistical weight corresponding to its level of importance, as presented in Table 2.

The weighted sum is calculated with Eq. (5), where m is the number of meteorological parameters.

$$WS = \sum_{j=1}^{m} WF_j FS_j \tag{5}$$

To conduct the analysis and verify the accuracy of the long-term wind speed behavior in the RWY compared to the 10 years analyzed, the measurement-correlation-prediction method (MCP) was employed (Ali et al., 2018). This method encompasses techniques for characterizing long-term wind data at a particular site (Liléo et al., 2013), focusing specifically on the examination

**Table 1: Coordinates of the offshore study areas**

| Number | Location | Latitude | Longitude |
|--------|----------|----------|-----------|
| Zone 1 | Uribia, La Guajira | 12.211 | −71.995 |
| Zone 2 | Ciénaga, Magdalena | 11.189 | −74.3501 |
| Zone 3 | Barraquilla, Atlántico | 11.228 | −74.8591 |
| Zone 4 | Puerto Velero, Atlántico | 10.9902 | −75.0573 |
| Zone 5 | Galera Zamba, Bolívar | 10.818 | −75.266 |

**Table 2: RWY weighting factors in this study**

| WF | Minimum | Maximum | Weight |
|----|---------|---------|--------|
| WS | 50/100 | 75/100 | 60/100 |
| WD | 5/100 | 20/100 | 20/100 |
| T | 10/100 | 30/100 | 10/100 |
| AP | 10/100 | 15/100 | 10/100 |

of the Weibull scale to assess the wind resource in the study area. The Weibull probability density function (PDF) is given by Eq. (6).

$$f(v) = \left(\frac{k}{c}\right)\left(\frac{v}{c}\right)^{k-1} e^{-\left(\frac{v}{c}\right)^k} \quad (v > 0; k, c > 0) \tag{6}$$

Where $v$ is the wind speed measured in m/s, $k$ is the shape parameter, and $c$ is the scale parameter measured in m/s. The cumulative distribution function is defined by Eq. (7).

$$F(v) = 1 - e^{-\left(\frac{v}{c}\right)^k} \tag{7}$$

For the calculation of parameters k and c, the Maximum Likelihood Method (MLM) was selected from among various options. This choice was informed by the analysis conducted by Vega-Zuñiga et al. (2022), wherein the authors evaluated 11 methods recognized in the literature and concluded that MLM is one of the best for representing wind data distribution. The equations for k and c are given by Eqs. (8) and (9), respectively.

$$k = \left[\frac{\sum_{i=1}^{N} v_i^k \ln v_i}{\sum_{i=1}^{N} v_i^k} - \frac{1}{N} \sum_{i=1}^{N} \ln v_i\right]^{-1} \tag{8}$$

$$c = \left[\frac{1}{N} \sum_{i=1}^{N} v_i^k\right]^{\frac{1}{k}} \tag{9}$$

For the wind direction index, wind rose diagrams corresponding to the RWY and 10-year behavior were plotted to verify and compare their accuracy in assisting the estimation of energy that can be extracted from the wind site (Hampannavar et al., 2021). To evaluate the prediction accuracy of the meteorological indices (WS, WD, T and AP) and to understand how they perform compared to the actual values, the results are corroborated by statistical error parameters, calculated using Eqs. (10-13). These parameters include Mean Percentage Error (MPE), Mean Absolute Percentage Error (MAPE), Root Mean Square Error (RMSE) and Mean Absolute Error (MAE), which are widely used in the literature to determine the accuracy of predictions (Adaramola, 2012; Khair et al., 2017; Patchali et al., 2022).

$$MPE = \frac{1}{n} \sum_{i=1}^{n} \left(\frac{(LT_i - RWY_i)}{LT_i} * 100\right) \tag{10}$$

$$MAE = \sum_{i=1}^{n} \frac{|LT_i - RWY_i|}{n} \tag{11}$$

$$MAPE = \frac{1}{n} \sum_{i=1}^{n} \left(\left|\frac{LT_i - RWY_i}{LT_i}\right| * 100\right) \tag{12}$$

$$RMSE = \sqrt{\sum_{i=1}^{n} \frac{(LT_i - RWY_i)^2}{n}} \tag{13}$$

Where $LT_i$ y $RWY_i$ correspond to the $i$ th long-term (LT) values and variables generated for the RWY respectively; and $n$ is the total number of observations.

## 3. RESULTS

Finkelstein-Schafer statistics of wind speed and direction, temperature and atmospheric pressure for Zone 1 are presented in Tables 3-6. These tables show monthly variations, demonstrating that representative years vary for each of these indices. Table 7 presents the calculated wind speed weighted sums values for each month in Zone 1, while Table 8 shows the best cases that correspond to the minimum values for each month. This table presents the 12 TMYs along with their respective weighted sums of wind speed, from January to December. The selected years are the following: 2019, 2013, 2021, 2013, 2016, 2020, 2017, 2017, 2019, 2021, 2017, 2013 and 2014. The entire generated dataset can be consulted in the data availability section.

Figure 3 shows the results of the 12 TMYs, taking as reference the wind speed, which is the most representative and important parameter. These data are distributed over 10 years. In a yearly

**Table 3: Finkelstein-Schafer statistics for wind speed**

| Years | January | February | March | April | May | June | July | August | September | October | November | December |
|---|---|---|---|---|---|---|---|---|---|---|---|---|
| 2012 | 0.0117 | 0.0144 | 0.0089 | 0.0276 | 0.0077 | 0.0067 | 0.0105 | 0.0069 | 0.0117 | 0.0326 | 0.0105 | 0.0103 |
| 2013 | 0.0039 | 0.0026 | 0.0067 | 0.0061 | 0.0216 | 0.0058 | 0.0086 | 0.0086 | 0.0158 | 0.0151 | 0.0057 | 0.0095 |
| 2014 | 0.0201 | 0.0113 | 0.0052 | 0.0231 | 0.0066 | 0.0127 | 0.0245 | 0.0044 | 0.0126 | 0.0111 | 0.0096 | 0.0039 |
| 2015 | 0.0101 | 0.0095 | 0.0085 | 0.0149 | 0.0191 | 0.0238 | 0.0079 | 0.0082 | 0.0170 | 0.0118 | 0.0235 | 0.0416 |
| 2016 | 0.0087 | 0.0089 | 0.0107 | 0.0162 | 0.0046 | 0.0081 | 0.0077 | 0.0123 | 0.0147 | 0.0244 | 0.0345 | 0.0117 |
| 2017 | 0.0168 | 0.0212 | 0.0097 | 0.0053 | 0.0085 | 0.0097 | 0.0072 | 0.0100 | 0.0270 | 0.0094 | 0.0078 | 0.0072 |
| 2018 | 0.0098 | 0.0071 | 0.0048 | 0.0072 | 0.0117 | 0.0032 | 0.0062 | 0.0130 | 0.0147 | 0.0063 | 0.0159 | 0.0160 |
| 2019 | 0.0024 | 0.0120 | 0.0139 | 0.0075 | 0.0139 | 0.0098 | 0.0116 | 0.0057 | 0.0195 | 0.0124 | 0.0092 | 0.0075 |
| 2020 | 0.0214 | 0.0076 | 0.0131 | 0.0036 | 0.0229 | 0.0025 | 0.0073 | 0.0084 | 0.0151 | 0.0108 | 0.0114 | 0.0117 |
| 2021 | 0.0074 | 0.0065 | 0.0024 | 0.0054 | 0.0048 | 0.0185 | 0.0084 | 0.0044 | 0.0096 | 0.0181 | 0.0166 | 0.0077 |

**Table 4: Finkelstein-Schafer statistics for wind direction**

| Years | January | February | March | April | May | June | July | August | September | October | November | December |
|---|---|---|---|---|---|---|---|---|---|---|---|---|
| 2012 | 0.0018 | 0.0014 | 0.0022 | 0.0020 | 0.0025 | 0.0029 | 0.0010 | 0.0075 | 0.0048 | 0.0222 | 0.0078 | 0.0026 |
| 2013 | 0.0011 | 0.0014 | 0.0021 | 0.0010 | 0.0090 | 0.0011 | 0.0016 | 0.0022 | 0.0019 | 0.0071 | 0.0076 | 0.0011 |
| 2014 | 0.0024 | 0.0023 | 0.0013 | 0.0030 | 0.0031 | 0.0011 | 0.0031 | 0.0050 | 0.0066 | 0.0075 | 0.0063 | 0.0027 |
| 2015 | 0.0006 | 0.0040 | 0.0008 | 0.0018 | 0.0019 | 0.0016 | 0.0008 | 0.0026 | 0.0059 | 0.0029 | 0.0091 | 0.0075 |
| 2016 | 0.0009 | 0.0013 | 0.0015 | 0.0033 | 0.0026 | 0.0022 | 0.0011 | 0.0033 | 0.0016 | 0.0107 | 0.0127 | 0.0021 |
| 2017 | 0.0030 | 0.0025 | 0.0018 | 0.0027 | 0.0018 | 0.0007 | 0.0007 | 0.0021 | 0.0069 | 0.0043 | 0.0191 | 0.0022 |
| 2018 | 0.0022 | 0.0019 | 0.0037 | 0.0009 | 0.0043 | 0.0011 | 0.0010 | 0.0032 | 0.0024 | 0.0065 | 0.0078 | 0.0027 |
| 2019 | 0.0005 | 0.0017 | 0.0015 | 0.0009 | 0.0024 | 0.0007 | 0.0017 | 0.0023 | 0.0212 | 0.0068 | 0.0110 | 0.0014 |
| 2020 | 0.0028 | 0.0013 | 0.0017 | 0.0015 | 0.0020 | 0.0023 | 0.0006 | 0.0033 | 0.0045 | 0.0068 | 0.0055 | 0.0024 |
| 2021 | 0.0021 | 0.0032 | 0.0021 | 0.0015 | 0.0041 | 0.0033 | 0.0012 | 0.0030 | 0.0060 | 0.0062 | 0.0079 | 0.0020 |

**Table 5: Finkelstein-Schafer statistics for temperature**

| Years | January | February | March | April | May | June | July | August | September | October | November | December |
|---|---|---|---|---|---|---|---|---|---|---|---|---|
| 2012 | 0.0016 | 0.0049 | 0.0018 | 0.0005 | 0.0014 | 0.0003 | 0.0008 | 0.0005 | 0.0006 | 0.0017 | 0.0010 | 0.0011 |
| 2013 | 0.0009 | 0.0010 | 0.0011 | 0.0006 | 0.0006 | 0.0007 | 0.0006 | 0.0005 | 0.0007 | 0.0008 | 0.0014 | 0.0014 |
| 2014 | 0.0011 | 0.0029 | 0.0004 | 0.0011 | 0.0011 | 0.0016 | 0.0006 | 0.0011 | 0.0016 | 0.0007 | 0.0003 | 0.0010 |
| 2015 | 0.0007 | 0.0037 | 0.0006 | 0.0016 | 0.0031 | 0.0011 | 0.0021 | 0.0014 | 0.0004 | 0.0005 | 0.0010 | 0.0005 |
| 2016 | 0.0007 | 0.0027 | 0.0022 | 0.0022 | 0.0030 | 0.0023 | 0.0012 | 0.0009 | 0.0002 | 0.0006 | 0.0008 | 0.0008 |
| 2017 | 0.0009 | 0.0005 | 0.0014 | 0.0019 | 0.0014 | 0.0008 | 0.0013 | 0.0010 | 0.0008 | 0.0003 | 0.0002 | 0.0005 |
| 2018 | 0.0023 | 0.0020 | 0.0014 | 0.0005 | 0.0011 | 0.0022 | 0.0021 | 0.0026 | 0.0012 | 0.0018 | 0.0014 | 0.0035 |
| 2019 | 0.0014 | 0.0012 | 0.0020 | 0.0005 | 0.0008 | 0.0008 | 0.0009 | 0.0005 | 0.0014 | 0.0018 | 0.0010 | 0.0022 |
| 2020 | 0.0023 | 0.0042 | 0.0012 | 0.0016 | 0.0010 | 0.0017 | 0.0026 | 0.0024 | 0.0021 | 0.0016 | 0.0009 | 0.0009 |
| 2021 | 0.0006 | 0.0010 | 0.0006 | 0.0022 | 0.0010 | 0.0004 | 0.0006 | 0.0005 | 0.0004 | 0.0014 | 0.0006 | 0.0002 |

**Table 6: Finkelstein-Schafer statistics for atmospheric pressure**

| Years | January | February | March | April | May | June | July | August | September | October | November | December |
|---|---|---|---|---|---|---|---|---|---|---|---|---|
| 2012 | 0.0018 | 0.0005 | 0.0021 | 0.0012 | 0.0040 | 0.0017 | 0.0022 | 0.0004 | 0.0020 | 0.0009 | 0.0008 | 0.0075 |
| 2013 | 0.0010 | 0.0022 | 0.0034 | 0.0008 | 0.0013 | 0.0017 | 0.0004 | 0.0012 | 0.0016 | 0.0011 | 0.0004 | 0.0032 |
| 2014 | 0.0012 | 0.0031 | 0.0009 | 0.0012 | 0.0009 | 0.0015 | 0.0024 | 0.0012 | 0.0010 | 0.0012 | 0.0019 | 0.0047 |
| 2015 | 0.0007 | 0.0011 | 0.0024 | 0.0008 | 0.0018 | 0.0006 | 0.0013 | 0.0017 | 0.0028 | 0.0003 | 0.0011 | 0.0072 |
| 2016 | 0.0007 | 0.0030 | 0.0013 | 0.0029 | 0.0008 | 0.0020 | 0.0010 | 0.0008 | 0.0030 | 0.0037 | 0.0033 | 0.0032 |
| 2017 | 0.0023 | 0.0019 | 0.0010 | 0.0018 | 0.0004 | 0.0011 | 0.0005 | 0.0001 | 0.0007 | 0.0012 | 0.0028 | 0.0030 |
| 2018 | 0.0043 | 0.0060 | 0.0027 | 0.0034 | 0.0015 | 0.0021 | 0.0012 | 0.0035 | 0.0017 | 0.0026 | 0.0016 | 0.0011 |
| 2019 | 0.0015 | 0.0007 | 0.0004 | 0.0025 | 0.0019 | 0.0007 | 0.0003 | 0.0003 | 0.0005 | 0.0010 | 0.0010 | 0.0089 |
| 2020 | 0.0009 | 0.0019 | 0.0036 | 0.0034 | 0.0011 | 0.0006 | 0.0038 | 0.0017 | 0.0010 | 0.0015 | 0.0009 | 0.0046 |
| 2021 | 0.0020 | 0.0013 | 0.0009 | 0.0017 | 0.0026 | 0.0013 | 0.0005 | 0.0013 | 0.0019 | 0.0014 | 0.0035 | 0.0040 |

**Table 7: Wind speed weighted sums of the Finkelstein-Schafer statistics**

| Years | January | February | March | April | May | June | July | August | September | October | November | December |
|---|---|---|---|---|---|---|---|---|---|---|---|---|
| 2012 | 0.0042 | 0.0053 | 0.0037 | 0.0078 | 0.0039 | 0.0029 | 0.0036 | 0.0038 | 0.0048 | 0.0144 | 0.0050 | 0.0054 |
| 2013 | 0.0017 | 0.0018 | 0.0033 | 0.0021 | 0.0081 | 0.0023 | 0.0028 | 0.0031 | 0.0050 | 0.0060 | 0.0038 | 0.0038 |
| 2014 | 0.0062 | 0.0049 | 0.0020 | 0.0071 | 0.0029 | 0.0042 | 0.0076 | 0.0029 | 0.0054 | 0.0051 | 0.0045 | 0.0031 |
| 2015 | 0.0030 | 0.0046 | 0.0031 | 0.0048 | 0.0065 | 0.0068 | 0.0030 | 0.0035 | 0.0065 | 0.0039 | 0.0087 | 0.0142 |
| 2016 | 0.0028 | 0.0040 | 0.0039 | 0.0061 | 0.0028 | 0.0037 | 0.0028 | 0.0043 | 0.0049 | 0.0099 | 0.0128 | 0.0044 |
| 2017 | 0.0057 | 0.0065 | 0.0035 | 0.0029 | 0.0030 | 0.0031 | 0.0024 | 0.0033 | 0.0089 | 0.0038 | 0.0075 | 0.0032 |
| 2018 | 0.0046 | 0.0043 | 0.0031 | 0.0030 | 0.0047 | 0.0022 | 0.0026 | 0.0056 | 0.0050 | 0.0043 | 0.0067 | 0.0058 |
| 2019 | 0.0015 | 0.0039 | 0.0045 | 0.0029 | 0.0048 | 0.0030 | 0.0036 | 0.0022 | 0.0107 | 0.0055 | 0.0055 | 0.0050 |
| 2020 | 0.0068 | 0.0037 | 0.0049 | 0.0025 | 0.0068 | 0.0018 | 0.0036 | 0.0040 | 0.0057 | 0.0052 | 0.0047 | 0.0049 |
| 2021 | 0.0030 | 0.0030 | 0.0015 | 0.0027 | 0.0031 | 0.0059 | 0.0027 | 0.0023 | 0.0045 | 0.0068 | 0.0072 | 0.0035 |

**Table 8: Minimum value of weighted sums for wind speed, 12 selected TMMs**

| | January | February | March | April | May | June | July | August | September | October | November | December |
|---|---|---|---|---|---|---|---|---|---|---|---|---|
| Year | 2019 | 2013 | 2021 | 2013 | 2016 | 2020 | 2017 | 2019 | 2021 | 2017 | 2013 | 2014 |
| WS | 0.0015 | 0.0018 | 0.0015 | 0.0021 | 0.0028 | 0.0018 | 0.0024 | 0.0022 | 0.0045 | 0.0038 | 0.0038 | 0.0031 |

**Figure 3:** Selection of the 12 TMMs for RWY generation with the wind speed index
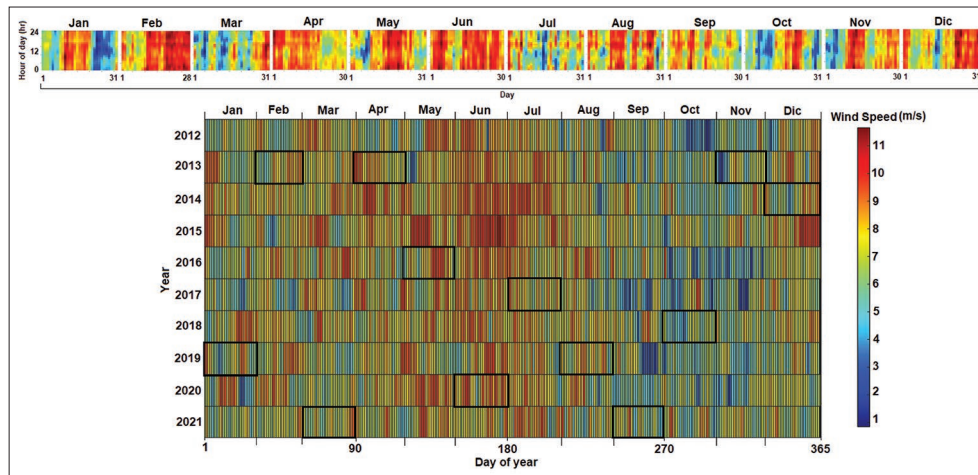


individual analysis, it was found that the years 2021 (March and September), 2019 (January and August) and 2013 (April and November) contributed the highest number of typical years. On the other hand, the years 2012, 2015 and 2018 were not part of the generation of the RWY set, since the weighted wind speed values of these years was not the minimum among the 10 years that were analyzed.

Figure 4 shows the behavior of the cumulative distribution function (CDF) calculated for the meteorological parameters, covering WS, WD, T and AP, over the 10 years closest to the long-term projection corresponding to the selected months in RWY. It is observed that there is concordance between the short-term data and the long-term data, reflecting a typical distribution. The comparisons are detailed in Figure 5. The differences between RWY and the long-term measurements are minimal.

The average monthly profile of WS is presented in Figure 5a, where the behavior of the long-term average is observed, compared to the RWY generated, the average wind speed was the highest in June with 8.24 m/s and 8.21 m/s for both cases respectively, and the lowest in October with 5.60 m/s and 5.56 m/s. In Figure 5b, the comparative average behavior of the WD index is observed, where

the average orientations are between 70° and 85° for the long-term data and for the RWY between 70° and 95°. In Figure 5c, it is reported that the average temperatures are between 25°C and 29°C for both cases. The AP is shown in Figure 5d, where the average values are observed between the range of 100 kPa and 101 kPa.

By applying the MCP method through MLM, the results corresponding to the shape and scale factors were obtained, to verify the accuracy of the RWY comparing it to the long-term behavior of the 10 years. In Figure 6a, the adjustment of the Weibull distribution corresponding to the 10 years analyzed is presented, as k = 4.80; c = 7.65 m/s, with an average power density (WPD)= 246.21 W/m$^2$ and average WS = 7.01 m/s.

In Figure 6b, the adjusted RWY curve is observed giving as results k = 4.57; c = 7.65 m/s, the WPD = 246.64 W/m$^2$, and an average WS = 6.98 m/s. These results show a positive similarity relationship with the long-term results. The wind data analysis indicates that the RWY does correspond to a representative data set of the long-term behavior of the wind speed in the studied area.

In Figure 7a, the wind rose diagram was plotted for the long-term behavior (10 years), showing a tendency towards the east, with
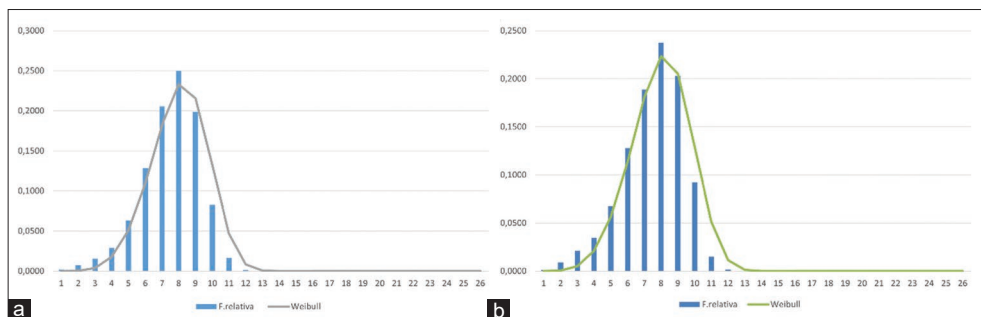
**Figure 4:** CDF comparison of meteorological parameters between short-term and long-term (a) WS, (b) WD, (c) T, and (d) AP
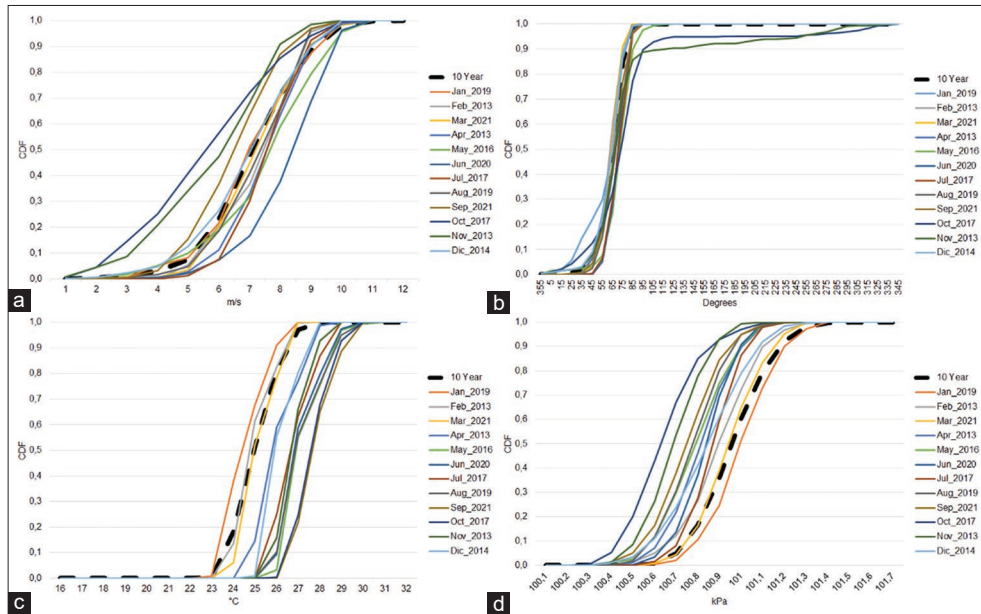


**Figure 5:** Mean monthly profiles of meteorological parameters between the short-term and the long-term (a) WS, (b) WD, (c) T, and (d) AP
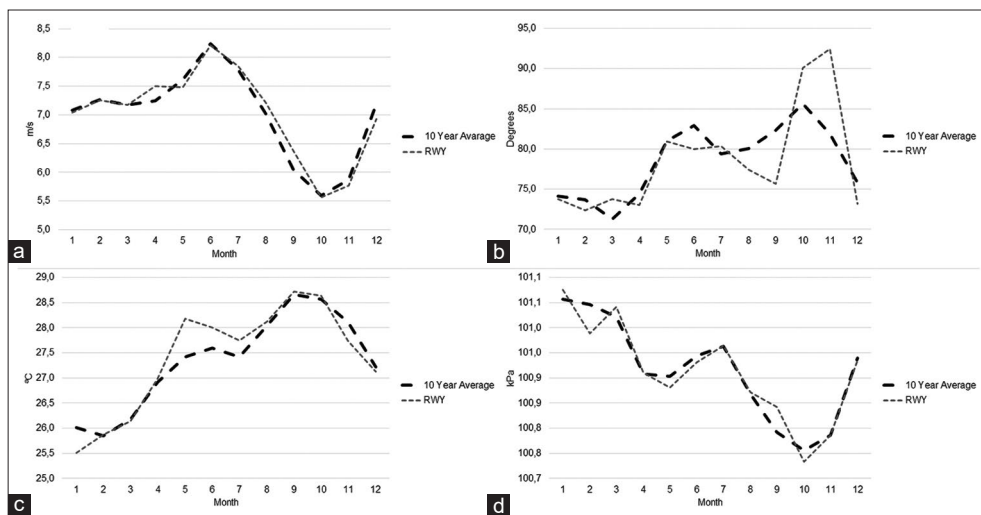


**Figure 6:** Weibull distribution (a) long-term 10 years, (b) RWY



wind speeds between 6 and 8 m/s equaling to 19.8% and between 8 and 10 m/s equaling to 26.4%. The wind rose diagram was plotted for the Reference Wind Year (RWY) in Figure 7b where it is observed that the wind blows from the east, with wind speeds above 6-8 m/s representing 20.4% and between 8 and 10 m/s with 27.2%.

When analyzing the results of the statistical error parameters presented in Table 9 for each meteorological parameter, concerning the WS, WD and T indices, negative values of MPE equal to −0.31%, −0.02% and −0.23% are observed, indicating that the RWY predictions tend to be slightly lower than the actual long-term values. Their proximity to zero suggests that the predictions are

**Figure 7:** Wind Rose Diagram (a) Long Term (10 years), (b) RWY
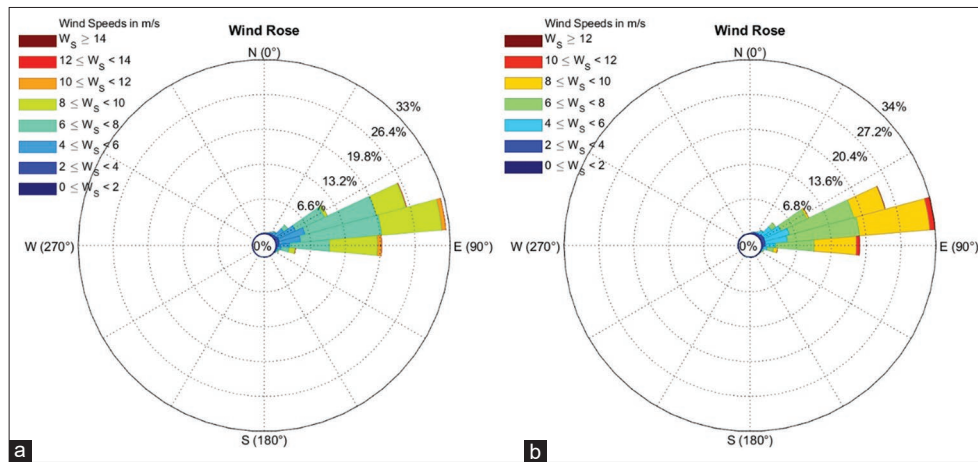


## Table 9: Results of statistical error parameters

| Metrics | WS (m/s) | WD (°) | T (°C) | AP (kPa) |
|---------|----------|--------|--------|----------|
| MAE | 0.12 | 3.03 | 0.23 | 0.0020 |
| MPE | −0.31% | −0.02% | −0.23% | 0.2% |
| MAPE | 1.80% | 3.77% | 0.86% | 0.02% |
| RMSE | 0.16 | 4.15 | 0.33 | 0.03 |

quite close in percentage terms. In the case of AP, a positive MPE close to zero, 0.2%, is recorded, indicating that the RWY estimates are slightly above the actual values, which also suggests that the predictions are quite close to the actual values in percentage terms.

The MAE indicates that, on average, the predictions exhibit an absolute error of 0.12, 3.03, 0.23 and 0.0020 relative to the actual values. A low value implies that the estimates are generally in close proximity to the long-term values. Notably, for WS and AP, an exceptionally high degree of proximity is observed, suggesting a high level of accuracy.

The RMSE, serving as another indicator of accuracy, yields results of 0.16, 4.15, 0.33 and 0.03, respectively. Minimal variance is observed in most cases, signifying low root mean square error and implying that the predictions are accurate, with small and consistent errors. The MAPE serves as a measure of average absolute percentage error between predictions and actual values, yielding results of 1.80%, 3.77%, 0.86% and 0.02% respectively. Low percentages suggest accuracy in percentage terms, with T and AP exhibiting particularly high accuracy.

## 4. CONCLUSIONS

Offshore wind energy has emerged as a promising resource for Colombia, particularly in the offshore Caribbean region, boasting class 7 winds with speeds exceeding 9 m/s. This presents significant opportunities for diversifying the energy matrix and transitioning towards more sustainable energy sources in the country. The methodology employed in this study is based on the traditional TMY generation method and the statistical Finkelstein-Schafer method. This approach has demonstrated accuracy and suitability for generating offshore wind specific RWY data. Statistical error parameters were applied to evaluate the precision of RWY

predictions against actual values, underscoring the efficacy of this approach. Overall, the findings suggest that the predictions are highly precise and closely align with long-term actual values, affirming the reliability of the results and their applicability in feasibility studies concerning offshore wind resource potential.

## 5. FUNDING

## REFERENCES

Abreu, E.F.M., Canhoto, P., Prior, V., Melicio, R. (2018), Solar resource assessment through long-term statistical analysis and typical data generation with different time resolutions using GHI measurements. Renewable Energy, 127, 398-411.

Adaramola, M.S. (2012), Estimating global solar radiation using common meteorological data in Akure, Nigeria. Renewable Energy, 47, 38-44.

Alargt, F.S., Khalifa, Y.M., Kharaz, A.H. (2021), Generation of a TMY for Tripoli City using the Finkelstein-Schafer Statistical Method. In: IECON Proceedings (Industrial Electronics Conference).

Ali, S., Lee, S.M., Jang, C.M. (2018), Forecasting the long-term wind data via Measure-Correlate-Predict (MCP) methods. Energies, 11(6), 11061541.

Alonso-Suárez, R., Bidegain, M., Abal, G., Modernell, P. (2019), Año Meteorológico Típico Para Aplicaciones de Energía Solar. Available from: https://www.colibri.udelar.edu.uy/jspui/handle/20.500.12008/7342

Amega, K., Laré, Y., Moumouni, Y., Bhandari, R., Madougou, S. (2022), Development of typical meteorological year for massive renewable energy deployment in Togo. International Journal of Sustainable Energy, 41(11), 1739-1758.

Arce, L., Bayne, S. (2020), Analysis of Offshore wind energy in Colombia: Current status and future opportunities. International Journal of Engineering Research, 9(11), 110277.

Attig-Bahar, F., Ritschel, U., Akari, P., Abdeljelil, I., Amairi, M. (2021), Wind energy deployment in Tunisia: Status, drivers, barriers and research gaps-A comprehensive review. Energy Reports, 7, 7374-7389.

Bautista Sánchez, C., Rojas Castellanos, K. (2019), Estudio de Prefactibilidad para el Desarrollo de un Parque Eólico Offshore Ubicado en la Ciudad de Cartagena-Bolívar [Universidad Militar Nueva Granada]. Available from: https://repository.unimilitar.edu.co/handle/10654/35847?show=full&locale-attribute=en

Bethel, B.J. (2021), Caribbean Sea Offshore wind energy assessment and forecasting. Journal of Marine Science and Application, 20(3), 558-571.

Bre, F., Fachinotti, V.D. (2016), Generation of typical meteorological years for the Argentine Littoral Region. Energy and Buildings, 129, 432-444.

Carvajal-Romo, G., Valderrama-Mendoza, M., Rodríguez-Urrego, D., Rodríguez-Urrego, L. (2019), Assessment of solar and wind energy potential in La Guajira, Colombia: Current status, and future prospects. Sustainable Energy Technologies and Assessments, 36, 100531.

Chan, A.L.S., Chow, T.T., Fong, S.K.F., Lin, J.Z. (2006), Generation of a typical meteorological year for Hong Kong. Energy Conversion and Management, 47(1), 87-96.

Costoya, X., de Castro, M., Santos, F., Sousa, M.C., Gómez-Gesteira, M. (2019), Projections of wind energy resources in the Caribbean for the 21st century. Energy, 178, 356-367.

De Meij, A., Vinuesa, J.F., Maupas, V., Waddle, J., Price, I., Yaseen, B., Ismail, A. (2016), Wind energy resource mapping of Palestine. Renewable and Sustainable Energy Reviews, 56, 551-562.

Ebrahimpour, A., Maerefat, M. (2010), A method for generation of typical meteorological year. Energy Conversion and Management, 51(3), 410-417.

Eikrem, K.S., Lorentzen, R.J., Faria, R., Stordal, A.S., Godard, A. (2023), Offshore wind farm layout optimization using ensemble methods. Renewable Energy, 216, 119061.

Gai, S., Zhang, X., Xie, J., Xiao, G., Liu, J. (2024), Comparison of typical meteorological year generation methods for building energy simulation in marine climate of China. Energy and Buildings, 304, 113845.

Gemignani, M., Rostegui, G., Salles, M.B.C., Kagan, N. (2017), Methodology for the Sizing of a Solar PV Plant: A Comparative Case. In: 2017 6th International Conference on Clean Electrical Power (ICCEP), Santa Margherita Ligure, Italy.

Hall, I.J., Prairie, R.R., Anderson, H.E., Boes, E.C. (1978), Generation of Typical Meteorological Years for 26 SOLMET Stations. Available from: https://www.osti.gov/biblio/7013202

Hampannavar, S., Patil, K.N., Manasani, S., Udaykumar, R.Y., Mandi, R.P., Nandakumar, C. (2021), Wind potential assessment for micropower generation in tropical wet climate of India. Lecture Notes in Electrical Engineering, 699, 337-348.

Himabindu, N., Hampannavar, S., Swapna, M., Patil, K.N. (2021), Wind Speed Assessment and Techno-economic analysis of a Community Microgrid in Warm and Humid Climate Zone of India. In: EUROCON 2021 - 19th IEEE International Conference on Smart Technologies, Proceedings. p531-536.

Kalogirou, S.A. (2003), Generation of typical meteorological year (TMY-2) for Nicosia, Cyprus. Renewable Energy, 28(15), 2317-2334.

Kambezidis, H.D., Psiloglou, B.E., Kaskaoutis, D.G., Karagiannis, D., Petrinoli, K., Gavriil, A., Kavadias, K. (2020), Generation of typical meteorological years for 33 locations in Greece: Adaptation to the needs of various applications. Theoretical and Applied Climatology, 141(3-4), 1313-1330.

Karamanski, S., Erfort, G. (2023), Wind energy supply profiling and Offshore potential in South Africa. Energies, 16(9), 16093668.

Khair, U., Fahmi, H., Al Hakim, S., Rahim, R. (2017), Forecasting error calculation with mean absolute deviation and mean absolute percentage error. Journal of Physics: Conference Series, 930(1), 012002.

Kotroni, V., Lagouvardos, K., Lykoudis, S. (2014), High-resolution model-based wind atlas for Greece. Renewable and Sustainable Energy Reviews, 30, 479-489.

Li, H., Yang, Y., Lv, K., Liu, J., Yang, L. (2020), Compare several methods of select typical meteorological year for building energy simulation in China. Energy, 209, 118465.

Liléo, S., Berge, E., Undheim, O., Klinkert, R., Bredesen, R.E., Vindteknikk, K. (2013), Long-term Correction of Wind Measurements State-of-the-art, Guidelines and Future Work Elforsk Report 13:18. Available from: https://energiforskmedia.blob.core.windows.net/media/19814/long-term-correction-of-wind-measurements-elforskrapport-2013-18.pdf

Maklad, Y. (2014), Generation of an annual typical meteorological solar radiation for Armidale NSWAustralia. International Organization of Scientific Research Journal of Engineering, 4, 41-45.

Mansani, S., Hampannavar, S., Patil, K.N., Narayan, K.V.L., Bairwa, B., Ayenew, E. (2021), Wind Speed Assessment of Three Climate Zones of Ethiopia. In: 3rd IEEE International Virtual Conference on Innovations in Power and Advanced Computing Technologies, i-PACT.

Minenergia. (2022), Energía Eólica Costa Afuera en Colombia. Available from: https://www.minenergia.gov.co/documents/5857/presentacion-hdre%c3%b3licos-v4.pdf

Ohunakin, O.S., Adaramola, M.S., Oyewola, O.M., Fagbenle, R.O. (2013), Generation of a typical meteorological year for North-East, Nigeria. Applied Energy, 112, 152-159.

Ospino-Castro, A., Robles-Algarín, C., Mangones-Cordero, A., Romero-Navas, S. (2023), An analytic hierarchy process based approach for evaluating feasibility of Offshore wind farm on the Colombian Caribbean Coast. International Journal of Energy Economics and Policy, 13(6), 64-73.

Patchali, T.E., Ajide, O.O., Matthew, O.J., Salau, T.A.O., Oyewola, O.M. (2022), Generation of meteorological year for the assessment of photovoltaic systems performance in Togo, West Africa. Scientific African, 16, e01171.

Pusat, S., Ekmekçi, I., Akkoyunlu, M.T. (2015), Generation of typical meteorological year for different climates of Turkey. Renewable Energy, 75, 144-151.

Pusat, S., Karagöz, Y. (2021), A new reference wind year approach to estimate long term wind characteristics. Advances in Mechanical Engineering, 13(5), 1-7.

Rodríguez, F., Castro, A., Marín, F., Roldán, G., Viteri Moya, F. (2019), Typical meteorological year based on the precipitation of Nanegalito and Pacto-Ecuador. Enfoque UTE, 10(1), 197-204.

Rueda-Bayona, J.G., Guzmán, A., Eras, J.J.C., Silva-Casarín, R., Bastidas-Arteaga, E., Horrillo-Caraballo, J. (2019), Renewables energies in Colombia and the opportunity for the offshore wind technology. Journal of Cleaner Production, 220, 529-543.

Skeiker, K. (2004), Generation of a typical meteorological year for Damascus zone using the Filkenstein-Schafer statistical method. Energy Conversion and Management, 45(1), 99-112.

Soto Gutiérrez, J.J. (2016), Desarrollo de la Energía Eólica en Colombia [Especialización en Gestión Ambiental, Universidad de América]. Available from: https://repository.uamerica.edu.co/bitstream/20.500.11839/624/1/5082005-2016-2-ga.pdf

The Renewables Consulting Group, ERM. (2022), Hoja de Ruta para el Despliegue de la Energía Eólica Costa Afuera en Colombia. Available from: https://www.minenergia.gov.co/es/micrositios/enlace-ruta-eolica-offshore

Vega-Zuñiga, S., Rueda-Bayona, J.G., Ospino-Castro, A. (2022), Evaluation of eleven numerical methods for determining Wei-bull parameters for wind energy generation in the Caribbean Region of Colombia. Mathematical Modelling of Engineering Problems, 9(1), 194-199.

Vergara, W., Deeb, A., Toba, N., Cramton, P., Leino, I. (2010), Wind Energy in Colombia A Framework for Market Entry. Available from: https://documents.worldbank.org/en/publication/documents-reports/documentdetail/766921468018592029/wind-energy-in-colombia-a-framework-for-market-entry

Xiang, L., Fu, X., Yao, Q., Zhu, G., Hu, A. (2024), A novel model for ultra-short term wind power prediction based on vision transformer. Energy, 294, 130854.